



Mitral Regurgitation Quantification from Multi-channel Ultrasound Images via Deep Learning

Keming Tang^{1,2,3}, Zhenyi Ge⁴, Rongbo Ling^{1,2,3}, Jun Cheng^{1,2,3},
Wufeng Xue^{1,2,3(✉)}, Cuizhen Pan^{4(✉)}, Xianhong Shu⁴, and Dong Ni^{1,2,3}

¹ National-Regional Key Technology Engineering Laboratory for Medical
Ultrasound, School of Biomedical Engineering, Shenzhen University Medical School,
Shenzhen University, Shenzhen, China

² Medical Ultrasound Image Computing (MUSIC) Laboratory,
Shenzhen University, Shenzhen, China

³ Marshall Laboratory of Biomedical Engineering,
Shenzhen University, Shenzhen, China

xuewf@szu.edu.cn

⁴ Department of Echocardiography, Shanghai Institute of Cardiovascular disease,
Zhongshan Hospital, Fudan University, Shanghai, China
pan.cuizhen@zs-hospital.sh.cn

Abstract. Mitral regurgitation (MR) is the most common heart valve disease. Prolonged regurgitation can cause changes in the heart size, lead to impaired systolic and diastolic capacity, and even threaten life. In clinical practice, MR is evaluated by the proximal isovelocity surface area (PISA) method, where manual measurements of the regurgitation velocity and the value of PISA radius from multiple ultrasound images are required to obtain the mitral regurgitant stroke volume (MRSV) and effective regurgitant orifice area (EROA). In this paper, we propose a fully automatic method for MR quantification, which follows the pipeline of ECG-based cycle detection, Doppler spectrum segmentation, PISA radius segmentation, and MR quantification. Specifically, for the Doppler spectrum segmentation, we proposed a novel adaptive-weighting multi-channel segmentation network, PISA-net, to accurately identify the upper and lower contours of the PISA radius from a pair of coupled M-mode PISA image and corresponding M-mode decolored image. Using the complementary information of the two coupled images and combining with the spatial attention module, the proposed PISA-net can well identify the contours of the PISA radius and therefore lead to accurate quantification of MR parameters. To the best of our knowledge, this is the first study of automatic MR quantification. Experimental results demonstrated the effectiveness of the whole pipeline, especially the PISA-net for PISA radius segmentation. The full method achieves a high Pearson correlation of 0.994 for both MRSV and EROA, implying its great potential in the clinical application of MR diagnosis.

Keywords: Mitral regurgitation · Multi-channel · Segmentation

1 Introduction

Mitral regurgitation (MR) is the most common heart valve disease. The incidence increases significantly with age, with more than 13% prevalence in the population over 75 years old [12]. MR is a mitral valve lesion caused by organic or functional changes in the mitral leaflets, annulus, papillary muscles, or tendon cords. Prolonged regurgitation can cause changes in the heart size, and lead to impaired systolic and diastolic capacity, resulting in decreased cardiac function and even being life-threatening.

In the clinical diagnosis of MR, physicians assess the extent of MR by calculating the effective regurgitant orifice area (EROA) and mitral regurgitant stroke volume (MRSV) of MR patients from ultrasound images, including continuous wave Doppler images (CW) and color Doppler image (CD). The most commonly applied method for calculating EROA and MRSV uses measurements derived from the proximal isovelocity surface area (PISA) method [3, 4, 6, 18, 20]. It is a hemispherical isovelocity surface that points to the regurgitant blood flow at the valve orifice when accelerated, and this phenomenon is used for quantitative evaluation of regurgitant flow. Bargiggia et al. [1] used the single-point PISA method to estimate MRSV in the routine clinical diagnosis. However, the underlying assumption that the size of the regurgitant orifice (during systole) is constant can not be held, therefore usually leads to overestimation or underestimation of MRSV. To account for the dynamic variation, Chen et al. [2] proposed an M-mode PISA and Enriquez-Sarano et al. [5] proposed a Serial PISA. However, the average orifice area used in M-mode PISA and the temporal sampling in Serial PISA undermine the accuracy of the estimation. Militaru et al. [11] sought to evaluate the accuracy of a new postprocessing software to quantify MR that allows semi-automated computation of MR severity from 3D color Doppler transesophageal echocardiographic images. The method significantly underestimates MR and can only measure MRSV, ignoring other parameters like EROA, which may be a better predictor. Singh et al. [15] evaluated a semi-automated method using 3D color data sets of MR to quantify MRSV and transmitral dynamic flow curves. However, The EROA is subject to inaccuracy in the setting of altered tissue or color gain, which cannot extrapolate to the effectiveness of this method. Modified PISA [9, 14, 16] was proposed later to calculate more accurate MRSV and EROA with continued temporal curves of the blood velocity and the PISA radius obtained from multi-channel ultrasound images, including CW image, two-dimensional M-mode ultrasound image (M2D) and M-mode color Doppler image (MCD). However, it is still time-consuming and laborious to implement the method manually. In this paper, we aim to automatize this procedure, where automatic identification of the above-mentioned two curves during the regurgitation period is required.

Most of the existing methods for the automatic detection of Doppler image contours were based on noise reduction and boundary tracking algorithms. In [7, 17], classic image processing techniques such as low-pass filtering, thresholding, and edge detection were used. However, robustness and generalization in the presence of severe image artifacts cannot be guaranteed. A probabilistic,

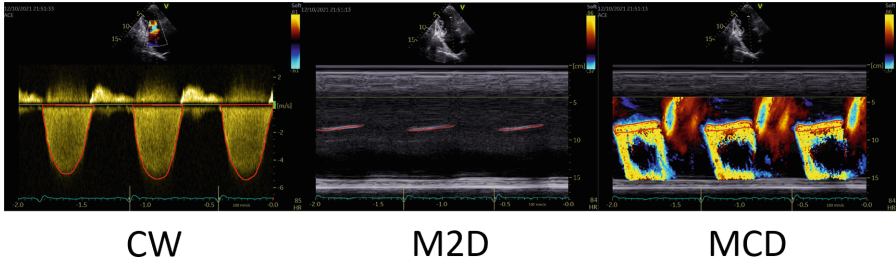


Fig. 1. Examples of the multi-channel ultrasound images, (1)continuous wave Doppler images (CW) are used to capture the blood velocity; (2)two-dimensional M-mode ultrasound images (M2D) provide the lower bound of the PISA radius; (3)M-mode color Doppler images (MCD) provide the upper bound of the PISA radius.

hierarchical, and discriminant(PHD) framework [21], was successfully applied to the automatic contour tracking of three kinds of Doppler blood flow images. Some related works have focused on model-based image segmentation algorithms. Indeed, knowing the expected shape can improve the tracking of velocity profiles. In the work of Wang et al. [19], a model-based feedback and adaptive weighted tracking algorithm was proposed. The algorithm combines a nonparametric statistical comparison of image intensities to estimate the edges of noisy impulse Doppler signals and a statistical shape model learned during manual tracking of the contours using. As for the M-mode ultrasound images, there is no existing automatic analysis method yet. In this method, we aim to estimate MRSV and EROA from multi-channel ultrasound images: CW, M2D, and MCD images (as illustrated in Fig. 1). While the CW image is used to estimate the blood velocity, the M2D and MCD images are used to estimate the contour of the PISA radius. Besides the presence of heavy noise in the images, a non-trivial challenge is that the M2D image is good at capturing the lower bound of the PISA radius, while the upper bound of the MCD image. To estimate the contour of the PISA radius, complementary information should be well extracted from the two images.

The contribution of the paper can be summarized as follows: First, we propose the first fully automatic pipeline for MR quantification from multi-channel ultrasound images based on the modified PISA method. The pipeline includes ECG-based cycle detection, Doppler spectrum segmentation, PISA radius segmentation, and MR quantification; Secondly, we propose a novel adaptive-weighting multi-channel segmentation network, PISA-net, to identify the lower and upper contours of the PISA radius from the complementary and coupled images, i.e., M2D and MCD. The network can adaptively select the related information of the corresponding input image and lead to an accurate estimation of the radius contour. Thirdly, after calculation based on the modified method, our method achieves accurate estimation of MRSV and EROA, with a Pearson correlation of 0.994 with the ground truths for both MR parameters.

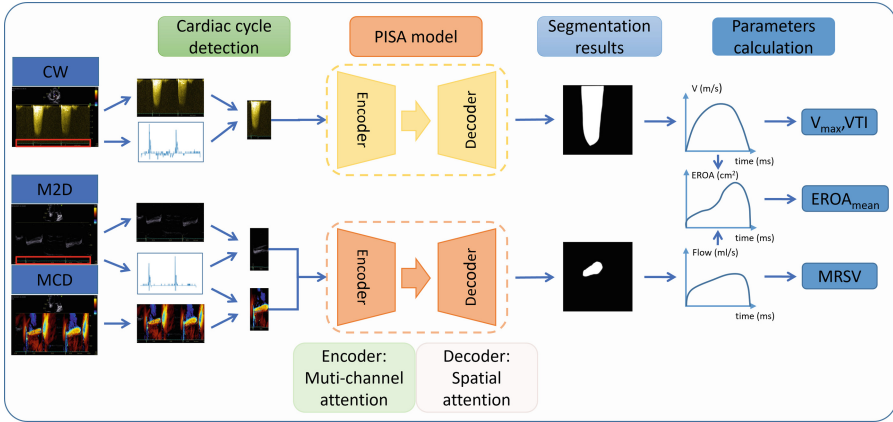


Fig. 2. Overview of the framework for MR quantification. This framework predicts four parameters from multi-channel ultrasound images: the peak flow velocity (V_{max}), the flow velocity time integral (VTI), the mitral regurgitant stroke volume (MRSV), and the effective regurgitant orifice area (EROA).

2 Method

The overview of the proposed method illustrate in Fig. 2, and it contains three stages: (1) ECG-based cycle detection, (2) Doppler spectrum and PISA radius segmentation, and (3) MR quantification. The details of the proposed pipeline are as follows.

2.1 ECG-Based Cardiac Cycle Detection

Multiple cardiac cycles appear in the above-mentioned ultrasound images (Fig. 1). The first step in the pipeline is to segment the image content of each cycle, as shown in Fig. 2. The regions of interest in these ultrasound images, i.e., the blood spectrum in CW, and the texture content in the M2D and MCD are first cropped out according to the meta information of the DICOM file. The ECG signals as shown at the bottom of these images are first extracted and then used to segment the cropped images into multiple single-cycle images.

2.2 Doppler Spectrum and PISA Radius Segmentation

We proposed the PISA-net to obtain the Doppler spectrum and PISA radius segmentation from multi-channel images. The architecture of the PISA-net is shown in Fig. 3. We employ a classic U-net structure (Fig. 3(a)) as the baseline model for our task. Considering the above-mentioned challenges, we introduce the adaptive-weighting strategy for features from different images in the encoder so that PISA-net can learn which image should be used to extract the low-level

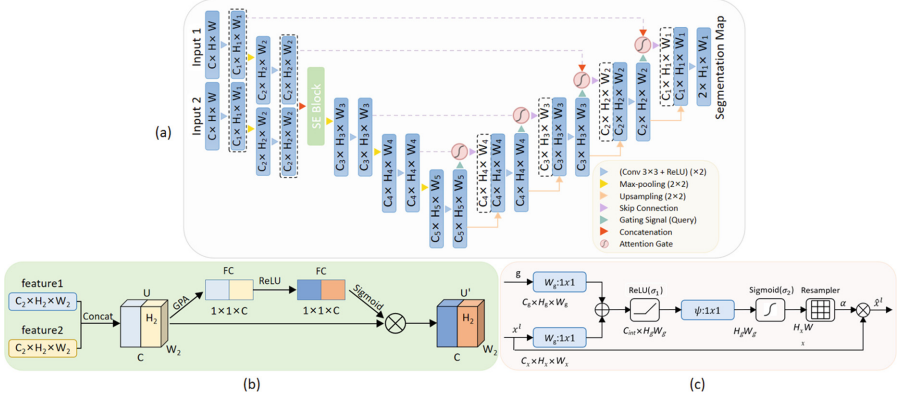


Fig. 3. Overview of the proposed PISA-net. (a) the architecture of PISA-net. (b) Squeeze-and-excitation(SE) block with attention mechanism on channel features. (c) Attention gate(AG) with attention mechanism on spatial features.

features for the lower and upper bounds of the PISA radius, respectively. To alleviate the effect of the heavy noise in these images, we introduce spatial attention mechanisms for features of the decoder layers, so that the global context can be used to suppress local noisy features.

Adaptive-Weighting Multi-channel Attention. PISA radius segmentation requires complementary information of both M2D and MCD images, and may also be affected by the image quality. We utilize the SE block [8] to adaptively weight features from different image channels. The structure of the SE block is shown in Fig. 3(b). Convolution features from M2D and MCD images are first contacted together. Through the global average pooling (GPA), each feature channel is compressed into a real number that can represent the global information of the channel. Then two fully connected layers and a Sigmoid layer are used to generate weights for each feature channel. Finally, the contacted features of M2D and MCD are weighted according to the weight vector to adjust the relative importance.

Spatial Attention. The features in the decoder are further enhanced with a spatial attention mechanism using features of the encoder. In this work, the attention gate block [13] (as shown in Fig. 3(c)) is used. Let x^l be the output feature map from layer l of the encoder, and g represents features from the previous block. Then, these features are fused by the addition operation and passed through a Sigmoid function to calculate the spatial attention map. The feature map x^l is then multiplied with the attention map to the enhanced features \hat{x}^l , which makes the value of irrelevant regions smaller and the value of the target region larger, and therefore improves both the network prediction speed and the segmentation accuracy.

2.3 MR Quantification

As shown in Fig. 2, the Doppler spectrum segmentation result of the CW image represents the velocity curve of the blood flow $v(t)$ at time t in the PISA radius. From $v(t)$, the maximum velocity v_{max} and the velocity time integral VTI can be calculated. The PISA-net predicts the upper bound and the lower bound of the radius contour from the M2D and MCD images. The distance between the two bounds represents PISA radius $r(t)$, which can be used to quantify the regurgitant flow rate $F(t)$ and MRSV. Finally, EROA is calculated from the regurgitant flow rate $F(t)$ and the blood flow velocity $v(t)$. Detailed formulas are as follows:

$$F(t) = 2 \cdot \pi \cdot r^2(t) \cdot V_a \quad (1)$$

$$MRSV = \int_0^t F(t) dt = 2 \cdot \pi \cdot V_a \cdot \int_0^t r^2(t) dt \quad (2)$$

$$EROA(t) = \frac{F(t)}{v(t)} \quad (3)$$

$$EROA_{mean} = \frac{\int_0^T EROA(t) dt}{T} \quad (4)$$

where V_a is a constant representing the aliasing velocity, and T denotes the duration length of the regurgitation.

3 Experiment and Results

3.1 Experimental Configuration

We obtained Doppler ultrasound images of 205 MR patients from a local hospital, and 157 of them were collected by GE Vivide95 while the rest 48 were collected by PHILIPS CX50. For each patient, three images were included: CW, M2D, and MCD, as shown in Fig. 1. Data use declaration and acknowledgement: Our dataset was collected from Zhongshan Hospital, Fudan University. This study was approved by local institutional review boards. We divide these ultrasound images into a training dataset (159 patients) and a test dataset (46 patients). Among the test set, 45 patients had degenerative mitral regurgitation, and 1 had functional mitral regurgitation. All images were annotated by experienced doctors using the Pair annotation software package (<https://www.aipair.com.cn/en/>, Version 2.7, RayShape, Shenzhen, China) [10].

We used the Dice score to evaluate the segmentation accuracy, and the Pearson correlation coefficient (corr), mean absolute error (MAE), and mean relative error (MRE) to assess the performance of MR parameters estimation.

Our method was implemented using Pytorch 1.7.1 and trained on an NVIDIA A100 GPU. The size of the input image is $3 \times 256 \times 256$. The model was optimized by minimizing the binary cross-entropy loss function and using the Adam optimization algorithm. The learning rate was set as 0.001.

3.2 Results and Analysis

Effect of Adaptive Weighting and Multiple Channel. We test the effect of the adaptive weighting mechanism in PISA-net when placed in different positions of the encoder. Table 1 shows the segmentation performance for single inputs and multi-channel inputs, with the adaptive weighting in different layers. It can be drawn that 1)for both the spectrum segmentation and the PISA radius segmentation, the adaptive weighting performs best when placed after the second convolution block of the encoder; and 2) the multi-channel inputs for PISA radius segmentation do help improve the performance, implying that PISA-net can effectively make use of the complementary information in these images. Results in the third and fourth columns of Table 2 also validate this.

Table 1. Effect of the adaptive weighting and multiple channel inputs.

Image	layer1	layer2	layer3	layer4
CW	0.961	0.962	0.960	0.960
MCD	0.923	0.925	0.924	0.923
M2D+MCD	0.926	0.937	0.926	0.924

Table 2. Mean Dice of CW image input, MCD image input, and M2D and MCD inputs on the test set.

Method	CW	MCD	M2D+MCD
Unet	0.958	0.910	0.886
Unet+SE	0.958	0.911	0.918
Att-Unet	0.961	0.925	0.926
PISA-net	0.962	0.925	0.937

Segmentation Performance. We compared PISA-net with three different methods: Unet, Unet with SE block(Unet+SE), and Attention Unet(Att-Unet) with different images as the input, and the results are shown in Table 2. The proposed PISA-net achieves the best accuracy, while the Unet gets the lowest accuracy. When M2D and MCD are combined as the input, Unet+SE, Att-Unet, and PISA-net achieve better accuracy than that of single input MCD. These results demonstrate the effectiveness of multi-channel adaptive weighting and spatial attention. Figure 4 shows examples of the summation of the weights learned for features from M2D and MCD images, respectively. It can be observed that our method can learn the weights of the two images adaptively for different samples.

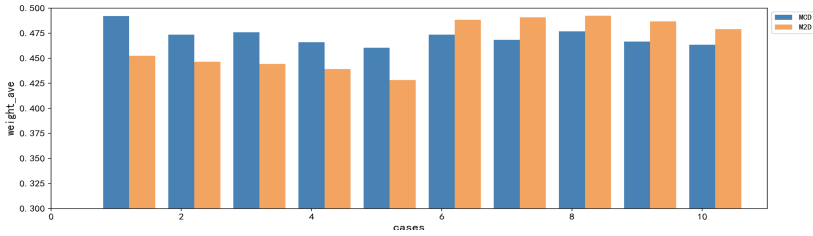
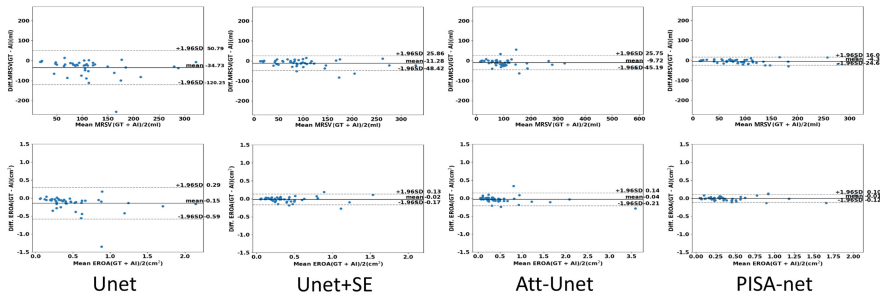


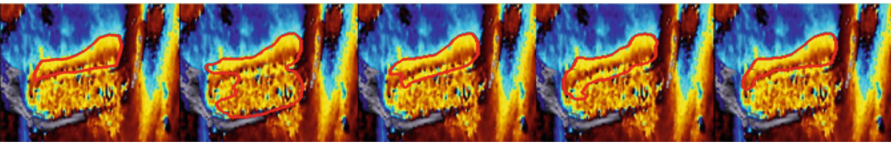
Fig. 4. Visualization of the average weights of the two inputs after using the SE block.

Table 3. Comparison of MR parameters quantification. The unit of MRE is %, For MAE, the unit of v_{max} is m/s, the unit of VTI is cm, the unit of MRSV is ml, the unit of $EROA_{mean}$ is cm^2 .

Method	Vmax			VTI			MRSV			EROA-mean		
	corr	MAE	MRE	corr	MAE	MRE	corr	MAE	MRE	corr	MAE	MRE
Unet	0.971	0.21	3.87	0.914	13.94	5.79	0.802	35.66	67.48	0.860	0.156	64.28
Unet+SE	0.894	0.20	3.70	0.930	19.96	8.63	0.960	14.63	18.12	0.981	0.054	15.05
Att-Unet	0.914	0.16	2.95	0.949	14.24	6.15	0.982	14.07	17.41	0.988	0.059	17.82
PISA-net	0.909	0.18	3.29	0.939	14.20	6.25	0.994	8.49	9.95	0.994	0.040	11.27



(a)



(b)

Fig. 5. (a) The MRSV and EROA calculated from the segmentation results of the four methods are compared with ground truth(GT). Bland-Altman plots show their bias. (b) Comparison of the segmentation results of a bad case in four methods.

Parameters Quantification. Table 3 is the comparison result for MR parameters quantification by different methods. PISA-net significantly outperforms the other methods for MRSV and EROA, with a Pearson correlation coefficient of 0.994 for both MR parameters. Figure 5(a) shows the Bland-Altman analysis of MRSV and EROA obtained. The PISA-net results in the least estimation bias. Figure 5(b) shows the segmentation results of a bad case for all four methods. PISA-net can still identify the lower and upper contours of the PISA radius from the complementary and coupled images accurately, showing the effectiveness of the adaptive weighting and the spatial attention.

4 Conclusion

In this work, we proposed the first fully automatic pipeline for MR quantification from multi-channel ultrasound images (CW, M2D, and MCD), based on the modified PISA method. An adaptive weighting mechanism and a spatial attention mechanism weighting were used to combine features of multi-channel inputs and enhance the local feature with a global context. Extensive experiments demonstrate that the proposed method is capable of delivering good segmentation results and excellent quantification of MR parameters, and has great potential in the clinical application of MR diagnosis.

Acknowledgement. The work is partially supported by the Natural Science Foundation of China (62171290), the Shenzhen Science and Technology Program (20220810145705001, JCYJ20190808115419619, SGDX20201103095613036), Medical Scientific Research Foundation of Guangdong Province (No. A2021370).

References

1. Bargiggia, G.S., et al.: A new method for quantitation of mitral regurgitation based on color flow doppler imaging of flow convergence proximal to regurgitant orifice. *Circulation* **84**, 1481–1489 (1991)
2. Chen, C., et al.: Noninvasive estimation of regurgitant flow rate and volume in patients with mitral regurgitation by doppler color mapping of accelerating flow field. *J. Am. Coll. Cardiol.* **21**(2), 374–83 (1993)
3. Dujardin, K.S., Enriquez-Sarano, M., Bailey, K.R., Nishimura, R.A., Seward, J.B., Tajik, A.J.: Grading of mitral regurgitation by quantitative doppler echocardiography: calibration by left ventricular angiography in routine clinical practice. *Circulation* **96**(10), 3409–15 (1997)
4. Enriquez-Sarano, M., Miller, F.A.J., Hayes, S.N., Bailey, K.R., Tajik, A.J., Seward, J.B.: Effective mitral regurgitant orifice area: clinical use and pitfalls of the proximal isovelocity surface area method. *J. Am. Coll. Cardiol.* **25**(3), 703–9 (1995)
5. Enriquez-Sarano, M., Sinak, L.J., Tajik, A.J., Bailey, K.R., Seward, J.B.: Changes in effective regurgitant orifice throughout systole in patients with mitral valve prolapse. a clinical study using the proximal isovelocity surface area method. *Circulation* **92**(10), 2951–2958 (1995)

6. Giesler, M., et al.: Color doppler echocardiographic determination of mitral regurgitant flow from the proximal velocity profile of the flow convergence region. *Am. J. Cardiol.* **71**(2), 217–24 (1993)
7. Greenspan, H., Shechner, O., Scheinowitz, M., Feinberg, M.: Doppler echocardiography flow-velocity image analysis for patients with atrial fibrillation. *Ultrasound Med. Biol.* **31**(8), 1031–40 (2005)
8. Hu, J., Shen, L., Albanie, S., Sun, G., Wu, E.: Squeeze-and-excitation networks. *IEEE Trans. Pattern Anal. Mach. Intell.* **42**, 2011–2023 (2017)
9. Hung, J.W., Otsuji, Y., Handschumacher, M.D., Schwammenthal, E., Levine, R.A.: Mechanism of dynamic regurgitant orifice area variation in functional mitral regurgitation: physiologic insights from the proximal flow convergence technique. *J. Am. Coll. Cardiol.* **33**(2), 538–45 (1999)
10. Liang, J., et al.: Sketch guided and progressive growing GAN for realistic and editable ultrasound image synthesis. *Med. Image Anal.* **79**, 102461 (2022)
11. Militaru, S., et al.: Validation of semiautomated quantification of mitral valve regurgitation by three-dimensional color doppler transesophageal echocardiography. *J. Am. Soc. Echocardiogr.* **33**(3), 342–354 (2020). <https://doi.org/10.1016/j.echo.2019.10.013>, <https://www.sciencedirect.com/science/article/pii/S0894731719311150>
12. Nkomo, V.T., Gardin, J.M., Skelton, T.N., Gottdiener, J.S., Scott, C.G., Enriquez-Sarano, M.: Burden of valvular heart diseases: a population-based study. *Lancet* **368**, 1005–1011 (2006)
13. Oktay, O., et al.: Attention U-Net: Learning where to look for the pancreas. *ArXiv abs/1804.03999* (2018)
14. Schwammenthal, E., Chen, C., Benning, F., Block, M., Breithardt, G., Levine, R.A.: Dynamics of mitral regurgitant flow and orifice area: physiologic application of the proximal flow convergence method: Clinical data and experimental testing. *Circulation* **90**, 307–322 (1994)
15. Singh, A., et al.: A novel approach for semiautomated three-dimensional quantification of mitral regurgitant volume reflects a more physiologic approach to mitral regurgitation. *J. Am. Soc. Echocardiogr.* **35**(9), 940–946 (2022). <https://doi.org/10.1016/j.echo.2022.05.005>, <https://www.sciencedirect.com/science/article/pii/S089473172200253X>
16. Sun, H.L., Wu, T.J., Ng, C.C., Chien, C.C., Huang, C.C., Chie, W.C.: Efficacy of oropharyngeal lidocaine instillation on hemodynamic responses to orotracheal intubation. *J. Clin. Anesth.* **21**(2), 103–7 (2009)
17. Tschirren, J., Lauer, R.M., Sonka, M.: Automated analysis of doppler ultrasound velocity flow diagrams. *IEEE Trans. Med. Imaging* **20**, 1422–1425 (2001)
18. Vandervoort, P.M., et al.: Application of color doppler flow mapping to calculate effective regurgitant orifice area. an in vitro study and initial clinical observations. *Circulation* **88**(3), 1150–1156 (1993)
19. Wang, Z.W., Slabaugh, G.G., Zhou, M., Fang, T.: Automatic tracing of blood flow velocity in pulsed doppler images. In: 2008 IEEE International Conference on Automation Science and Engineering, pp. 218–222 (2008)
20. Yamachika, S., et al.: Usefulness of color doppler proximal isovelocity surface area method in quantitating valvular regurgitation. *J. Am. Soc. Echocardiogr.* **10**(2), 159–168 (1997). [https://doi.org/10.1016/S0894-7317\(97\)70089-0](https://doi.org/10.1016/S0894-7317(97)70089-0), <https://www.sciencedirect.com/science/article/pii/S0894731797700890>
21. Zhou, S.K., et al.: A probabilistic, hierarchical, and discriminant framework for rapid and accurate detection of deformable anatomic structure. In: 2007 IEEE 11th International Conference on Computer Vision, pp. 1–8 (2007)